ELSEVIER

Chemical Engineering Journal 81 (2001) 69–81

Chemical Engineering Journal

www.elsevier.com/locate/cej

Liquid dispersion and gas holdup in packed bubble columns at atmospheric pressure

Peter Therning, Anders Rasmuson*

Department of Chemical Engineering, Design, Chalmers University of Technology, S-41296 Göteborg, Sweden

Received 26 June 1999; received in revised form 20 June 2000; accepted 23 June 2000

Abstract

The gas holdup and liquid axial dispersion coefficient are measured in two semibatch packed bubble columns, 0.154 and 0.200 m diameter for an air–water system, at atmospheric conditions. It is observed that the one-dimensional dispersion model does not give an accurate description of the tracer concentration profiles from a pulse injection. This is due to convective liquid flows inside the bed and poor radial mixing. The liquid circulation comprises an upward flow in the column core and a downward flow along the wall. Extension of the dispersion model to account for the convective recirculation is discussed. It is also seen that the radial mixing increases considerably in the pulsation flow regime and as a result of this; the dispersion coefficient reduces suddenly at the transition point between the bubble flow and the pulsation flow regime.

Keywords: Packed bubble columns; Liquid dispersion; Gas holdup; Liquid circulation

1. Introduction

Different kinds of bubble columns are frequently used in the chemical industry to perform gas–liquid reactions. Although this kind of equipment has been extensively investigated during the last decades, the number of published articles regarding the hydrodynamics in packed bubble columns is not as substantial. These works have considered, in particular, the influence of gas velocity, different packing, packing sizes, liquid flow, tower diameter and bed height.

An advantage, a packed bubble column can offer compared to a bubble column without any form of internals is a considerable reduction of the backmixing. The investigations have been carried out using RTD measurements and the backmixing is usually characterised by the axial dispersion coefficient obtained from the one-dimensional axial dispersion model. According to several authors, this model generally provides a suitable representation of backmixing in a packed bubble column. Katz [1], however, stated that the dispersion model is fairly a crude approximation. There are also some discrepancies in the effects of the gas velocity on the liquid dispersion coefficient. According to Shah et al. [2], it is generally believed that an increase in gas velocity increases the liquid dispersion coefficient.

In packed bubble columns, the gas holdup has been investigated by several authors for different kinds of packings (Stiegl and Shah [3]; Abraham and Sawant [4]; Niranjan and Pangarkar [5]). It is a well known fact that the gas holdup increases with increasing gas flow and that the packing size influences the gas holdup considerably. Several empirical correlations have been developed, but it is obvious that there is currently no universal correlation for predicting the gas holdup in packed bubble columns.

Turpin and Huntington [6] have identified three different flow regimes in packed bed reactors: the bubble flow, the pulse flow and the spray flow regimes. The bubble flow regime is characterised by individual gas bubbles flowing in an unbroken stream upwards in the bubble column. The pulse flow results in an increase in the gas flow to greater than 7–10 cm/s, and alternate portions of more dense and less dense phases pass through the column. The spray flow is where the gas is the continuous phase and the liquid acts as the dispersed phase

There are only a few studies discussing the different mixing phenomena in packed bubble columns. The aim of the present study is, therefore, to experimentally determine the gas holdup, the flow regimes and the liquid axial dispersion coefficient in a packed bubble column. The method used to determine the dispersion coefficient made it possible to avoid the problem with maldistribution of the tracer over the column cross-section. However, since this method requires a bubble column with no net flow of liquid the in-

* Corresponding author. Tel.: +46-31-772-29-40; fax: +46-31-81-46-20.
E-mail address: rasmus@kat.chalmers.se (A. Rasmuson).

1385-8947/01/$ – see front matter
PII: S1385-8947(00)00225-4

Nomenclature

A	cross-sectional area of bubble column (m^2)
C	concentration in the bubble column (kg/m^3 or mol/dm^3)
c	liquid pool concentration (kg/m^3 or mol/dm^3)
E	liquid dispersion coefficient, according to Eqs. (13) and (14) (m^2/s)
E_L	liquid dispersion coefficient (m^2/s)
K	exchange factor between up- and downflowing liquid (m^2/s)
L	height of the packed section (m)
M	amount of tracer in the packed section (kg)
q	the non-zero positive roots of Eq. (7)
R	radius of bubble column (m)
r	radial distance (m)
t	time (s)
U_G	superficial gas velocity (m/s)
U_L	superficial liquid velocity (m/s)
u	internal liquid velocity inside the bed (m/s)
V_G	gas volume in the packed section (m^3)
V_L	liquid volume in the packed section (m^3)
V_{Tot}	volume of bubble column (m^3)
v	liquid pool volume (m^3)
x	axial coordinate (m)

Greek symbols

α	the ratio between v/V_L
ε	voidage of packing
ε_G	gas phase holdup defined as V_G/V_{Tot}
ε_L	liquid phase holdup defined as V_L/V_{Tot}

Subscripts

A	the upper liquid pool
B	the liquid pool at the bottom
G	gas
inf	infinite time
L	liquid

Superscripts

d	downflow
u	upflow

vestigations were performed in a semibatch packed bubble column. This study also tries to describe the existing flow pattern and analyse the different mixing phenomena.

2. Experimental apparatus

The majority of the experiments were performed in a glass column with an internal diameter of 0.20 m, although some gas holdup measurements were made in a steel column with an internal diameter of 0.154 m. Both of the bubble columns were packed with 15 mm plastic Pall rings. The sparger design and the bed height of the two columns differ. The most important data of the two columns are collected in Table 1.

Table 1
Packed bubble column data

	Bubble column glass	Bubble column steel
Column diameter (m)	0.200	0.154
Hole diameter (mm)	2.0	1.5
Free hole area (%)	0.7	0.2
Bed height (m)	1.8	3.2
Bed voidage	0.86	0.88

The bubble columns were operated in a semibatch mode, i.e. they were operated continuously with respect to the gas flow but batchwise with respect to the liquid. The gas used was compressed air and the liquid was deionised water. In a packed column filled with 25 mm steel Pall rings, the air was humidified by water before entering the bubble column. In contrast to the glass column, the inlet gas stream to the steel column was not humidified. A grid was applied at the top of the bed of both bubble columns to prevent expansion of the packing materials.

In the glass column, an overflow was located 5 cm above the bed. This is shown in Fig. 1. A steel grid was located in the bottom section of the glass column, at a distance of 0.09 m above the perforated sparger, This is also shown in Fig. 1. The purpose of this arrangement was to ensure a satisfactory gas distribution. The space in the bottom section, i.e. the volume below the gas sparger, was totally free from liquid during operation.

In the steel column, the packing was applied directly on the sparger. A mass flow meter was installed at the gas outlet of the steel column. The range of gas flow measurements was restricted by the limitations of the mass flow meter and the gas supply system. The lowest gas flow rate that could be measured by the mass flow meter was unfortunately approximately 8.6 normal m^3/h. This means that the lowest superficial gas velocity at atmospheric pressure was approximately 0.13 m/s.

3. Methods

3.1. Gas holdup

The gas holdup is readily determined by measuring the height of the clear liquid after stopping the gas flow. The gas holdup is calculated by

$$\varepsilon_G = \frac{V_G}{V_{Tot}} \tag{1}$$

where V_{Tot} is the total volume of the packed bubble column without liquid pool and V_G the gas volume in the bed. The bubble column was filled with water to the packing height. When the gas was introduced the excess of liquid was entrained through the overflow, as shown in Fig. 1. When the

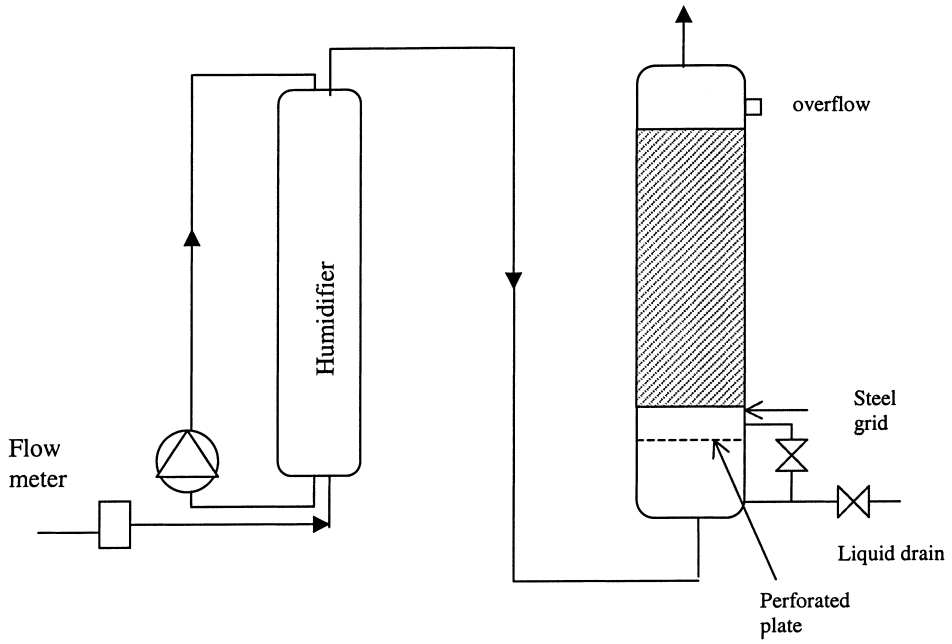

Fig. 1. Experimental setup for measurements in the packed bubble column.

gas flow was stopped, the clear liquid height was measured. In this case, for practical reasons the position of the overflow was about 0.05 m above the steel grid, whereas it was necessary to take this liquid volume into account when calculating the gas holdup. It was also necessary to consider the amount of liquid from the volume between the gas sparger and the lower steel grid. Some of this liquid volume was entrained up into the bed when starting the gas flow. Both of these liquid volumes are evaluated using the gas holdup values for an empty column. Due to the large total volume of the bubble column the errors that may arise from this estimation of the liquid volumes are more or less insignificant.

In the steel column, the gas holdup was measured using an overflow technique. The bubble column was filled with water to the same level as one of the sample points. The gas was introduced and, by measuring the volume of the entrained liquid, the gas holdup was calculated.

3.2. Liquid dispersion

As far as is known, in all the previous dispersion studies in semibatch packed bubble columns performed, the tracer has been added directly to the top of the bed. In co- or counter-current flow reactors, the tracer is generally injected to the liquid inlet stream whereas the response is measured at the outlet. One main disadvantage with these two methods is the difficulty in achieving a homogeneous dispersion of the tracer in the radial direction of the bed. To overcome this problem, Campos and Guedes de Carvalho [7] used a liquid pool above the packing in which a pulse of the tracer was introduced. By measuring the tracer concentration in the liquid pool as a function of time, the one-dimensional dispersion coefficient can be estimated.

The method used by Campos was used in this study. In contrast to Campos, samples were also taken from a point located approximately in the midsection of the packing. At this point, samples were taken at three different radial positions inside the bed; $r/R = 0$, 0.5, 0.9.

If the dispersion model is valid, the concentration of the tracer in the packed bed section could be described by

$$\frac{\partial C}{\partial t} = E_{\mathrm{L}} \frac{\partial^2 C}{\partial x^2} \tag{2}$$

where C is the tracer concentration and x the vertical position. It is assumed that the liquid pool can be considered as a well-stirred fluid, i.e. the tracer is instantaneously and completely mixed with the liquid after injection. This assumption is reasonable if the pool volume is not too large and when the mixing in an unpacked bubble column is rapid. If the mixing in the pool is rapid, the tracer concentration in the pool and the concentration of the tracer at the boundary ($x = 0$) can be considered as equal. It is also assumed that the tracer concentration reduction in the pool section is a result of dispersion alone. If all these assumptions are correct, Eq. (2) can be solved subject to the following boundary conditions:

$$C = 0 \text{ at } t = 0, \quad 0 \le x \le L \tag{3}$$

$$E_{\mathrm{L}} \frac{\partial C}{\partial x} = \frac{v}{A\varepsilon_{\mathrm{L}}} \frac{\partial c}{\partial t} \quad \text{at} \quad t > 0,\ x = 0 \tag{4}$$

$$\frac{\partial C}{\partial x} = 0 \quad \text{at} \quad t > 0,\ x = L \tag{5}$$

The solution is given, e.g. by Carslaw and Jaeger [8] and the concentration of the tracer within the packed bed section, $C(x, t)$, is expressed by

$$C(x,t) = C_{\text{inf}}\left(1 + \sum_{n=1}^{\infty} \frac{2(1+\alpha)\exp(-E_{\text{L}}q_n^2 t/L^2)\cos(q_n(L-x)/L)}{(1+\alpha+\alpha^2 q_n^2)\cos q_n}\right) \quad (6)$$

where C_{inf} is the tracer concentration after infinite time and q_n the non-zero positive roots of

$$\tan q_n = -\alpha q_n \quad (7)$$

and $\alpha = v/V_{\text{L}}$ is the ratio of the liquid volume in the pool to the liquid volume in the packed section.

When measuring the tracer concentration in the liquid pool, it is more convenient to express Eq. (6) as

$$\frac{M_t}{M_{\text{inf}}} = 1 - \sum_{n=1}^{\infty} \frac{2\alpha(1+\alpha)}{1+\alpha+\alpha^2 q_n^2} \exp\left(-\frac{E_{\text{L}} q_n^2 t}{L^2}\right) \quad (8)$$

where M_t is the total amount of tracer in the packed section at time t, and M_{inf} the corresponding quantity after infinite time.

In this work, the dispersion coefficients were evaluated using Eq. (8). The measured values were fitted to Eq. (8) by the least squares method.

In the experiments, a small portion of sulphuric acid was used as a tracer: approximately 100 ml of 4.0 g sulphuric acid per dm^3 was added to the liquid pool. The samples taken were analysed by measuring the electrical conductivity. For the concentrations measured in this study, the sulphuric acid concentration is proportional to the conductivity. The total sample volume for each run was approximately 150 ml.

The volume of the liquid pool, which varied between 6 and 10 dm^3, was determined by entraining liquid through the overflow. The liquid volume between the overflow and the packing was estimated by using the gas holdup values for an unpacked bubble column. The sum of these two volumes gives the liquid pool volume. The liquid volume in the packed bed section can be estimated from the liquid holdup.

4. Results and discussion

4.1. Gas holdup

The gas holdup values in this study, defined according to Eq. (1), are shown in Fig. 2 as a function of the superficial gas velocity. Results from both the steel and the glass column are presented in the figure.

As expected, the gas velocity increases the gas holdup. It is well known that packing prevents coalescence, and that there is no formation of larger bubbles as there is in an empty column operating in the churn-turbulent regime. The figure also shows that there is no significant difference in gas holdups due to the different bubble column constructions, e.g. sparger design and the internal diameter.

In a packed bubble column, the maximal bubble size is determined primarily by the packing size. Therefore, it could be suspected that the diameter of the column is of little

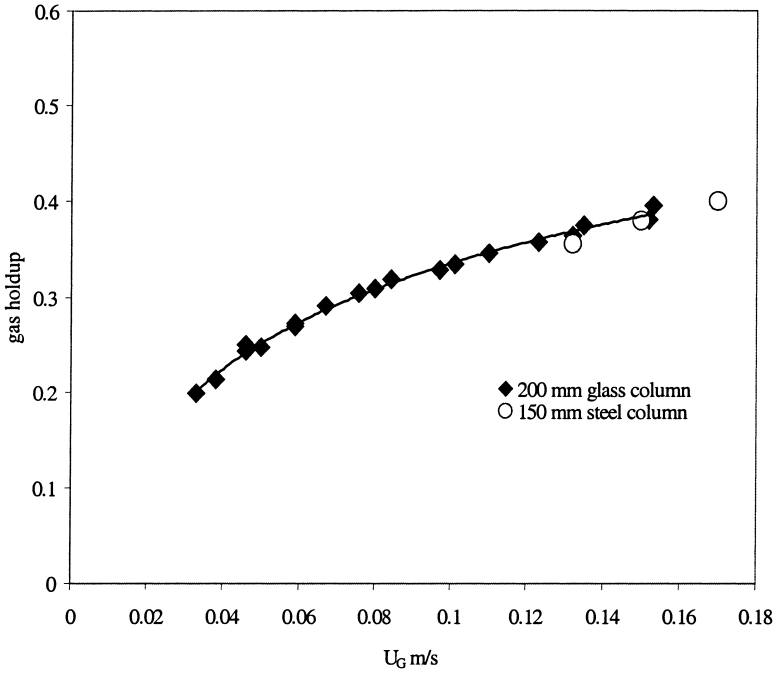

Fig. 2. Gas holdup as a function of superficial gas velocity in two different packed bubble columns.

importance. It is apparent that no correlation in the literature takes the column diameter into consideration. Niranjan and Pangarkar [5] reported identical gas holdups for two different columns of diameter 0.2 and 0.38 m. Sahay and Sharma [9] also used two different column diameters, 0.1 and 0.2 m for a variety of packings. These results are in agreement with the results obtained in this work.

4.2. Flow regimes

Two different flow regimes were observed visually at atmospheric conditions: namely, bubble and pulsation flow.

The pulses, which started at the lower part of the bed and moved upwards, were easily detected. These pulses form the pulsation flow region. In Fig. 3, the pulse frequencies have been plotted against the superficial gas velocity. The values of the pulse frequencies were determined by calculating the number of pulses during 1 min.

It can be seen that the flow regime transition point occurs at approximately 6–7 cm/s. Initially, the gas velocity influences the pulse frequencies modestly but at 12 cm/s, the pulse frequency increases dramatically. It was also observed that in the pulsation flow regime, the gas bubbles in the wall region were stagnant and only rose upwards together with the pulses. This phenomenon may be a result of an increased internal liquid velocity, and thus, an increased drag force between the gas bubbles and the down flowing liquid in the wall region. When the gas bubbles no longer move upwards in the wall region, the gas content and the gas velocity in the middle of the column have to increase due to the continuous supply of gas. According to this scenario, there are radial variations in the gas holdup.

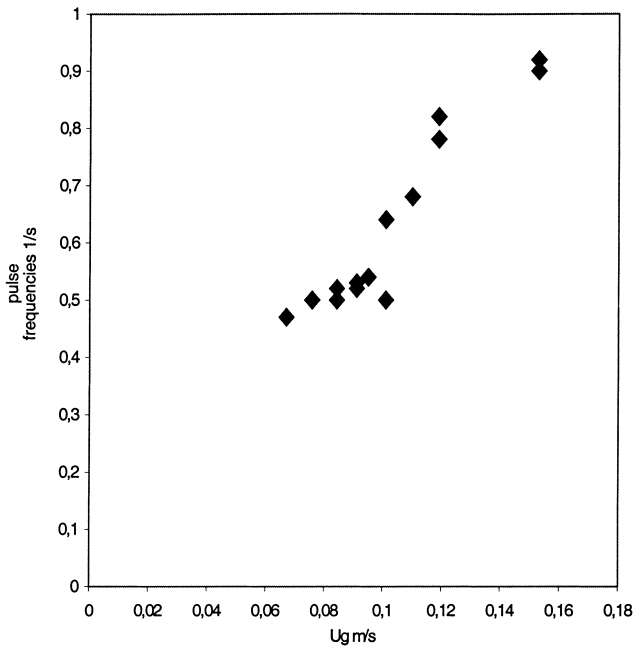

Fig. 3. The pulse frequencies as a function of superficial gas velocity. Bubble column diameter 0.2 m.

The pulses seem to be formed in a region approximately 30 cm above the gas sparger. This estimation is very rough, based on observations for both the glass and the steel column. By opening the lowest sample valve in the steel column, approximately 20 cm above the gas sparger, it could be observed that the liquid drained continuously. However, opening the other sample valves, showed that the liquid drained in a more discontinuous way: a period of flushing liquid is replaced by an air pulse and so forth. The lack of air pulses from the lowest sample point implies that no pulses are established in this region.

The transition point agrees well with data in the literature. Ramachadran and Chaudari [10] state that, for the transition points, the gas velocity is generally larger than 7–10 cm/s. It is interesting to note that the transition point in a packed bubble column occurs at a higher gas velocity compared to an unpacked bubble column, where the churn turbulent flow regimes starts at approximately 4 cm/s. This phenomenon can be explained by the fact that the packing effectively prevents the gas bubbles from coalescing.

4.3. Liquid axial dispersion

In Fig. 4, the results of the dispersion measurements are shown. It is evident that the dispersion coefficient depends on the gas velocity. It can also be seen that, contrary to what might be expected, the dispersion coefficient suddenly decreases at a gas velocity of approximately 6–7 cm/s. A further increase of the gas velocity results in an increase of the dispersion coefficient.

Several authors state that increasing the gas velocity increases the dispersion coefficient (Stiegel and Shah [3], Heilman and Hofman [11] and Hofman [12]). Stiegel and Shah [3] propose a correlation where the dispersion coefficient varies as $U_G^{0.16}$ for packing sizes of approximately 4 mm. For a bubble column packed with glass cylinders with a diameter of 3.8 mm and a length of 4.8 mm, Gelder and Westerterp [13] propose the exponent of U_G to be 0.313. Niranjan and Pangarkar [5] concluded that for packings with nominal dimensions of 25 mm and above, the influence of the gas velocity on the dispersion is considerable: the dispersion coefficient in this case varies approximately with $U_G^{0.3}$, while for smaller packings, the dispersion coefficient is almost independent of the gas velocity. Niranjan and Pangarkar [5] explained this by the fact that smaller packings suppress the bulk, and the probable cause of mixing in smaller packings is micro-turbulence. They suggest that for larger packings, mixing predominantly occurs by liquid circulation. Moreover, results obtained by Campos and Guedes de Carvalho [7], Carleton et al. [14] and Magnussen and Schumacher [15] give no rise in the dispersion when increasing the gas velocity.

As far as is known, only a few researchers have observed a local maximum in the value of E_L, as shown in Fig. 4. Hoogendorn and Lips [16] and Stemmerding [17] report a maximum in the dispersion for 13 mm ceramic Raschig

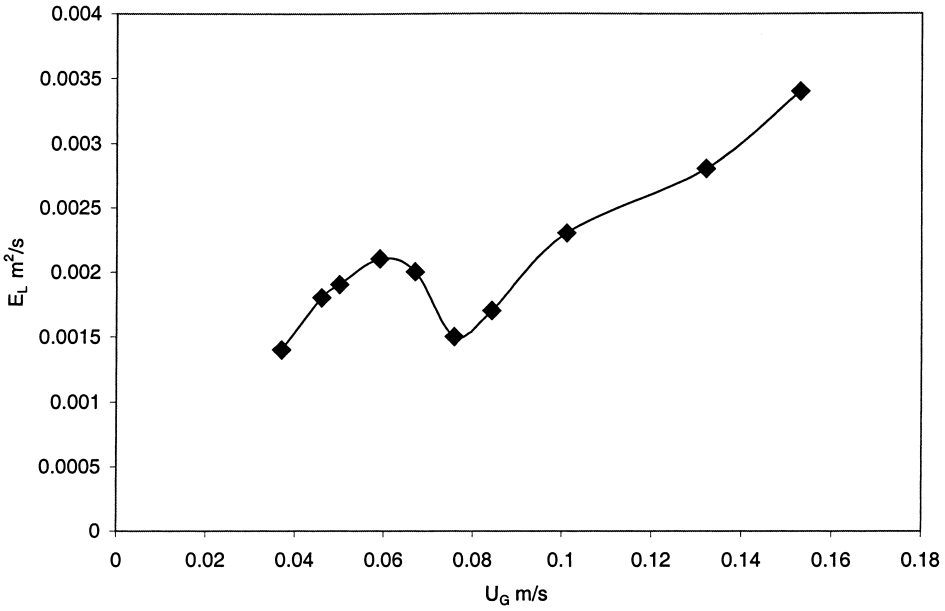

Fig. 4. The dispersion coefficient as a function of superficial gas velocity. Column diameter 0.2 m.

rings. Niranjan and Pangarkar [5] state, that these results are probably insignificant since the variations in E_L are small. Gelder and Westerterp [13] observed significant random variations in the dispersion data. Such scatter was explained, for example, by the random character of dispersion or by small fluctuations in feed rate. These authors concluded that the dispersion coefficient in the form of a Bodenstein number could not be determined with an error smaller than approximately 20%.

It is also worth noting that the influence of the bubble column diameter on the dispersion has only been considered in a few studies. One can neglect this influence provided the dispersion in the liquid phase is a diffusion like process, i.e. the dispersion model is valid. If a convective mechanism substantially contributes to the mixing, the influence of the column diameter may be an important parameter both in scale up and when comparing different correlations. Therefore, some dispersion measurements were carried out in the steel column, 0.154 m i.d. at a superficial gas velocity of 0.13 m/s. The dispersion coefficient in the steel column, $E_L = 0.017\,m^2/s$ was lower compared to approximately $0.028\,m^2/s$ in the larger 0.200 m column. Magnussen and Schumacher [15] observed a similar trend in their study. It is also well known that the dispersion coefficient in unpacked bubble columns is strongly affected by the column diameter. It is, therefore, obvious that the mixing mechanism occurring in a packed bubble column is not consistent with the basic condition of the dispersion model.

Fig. 5 shows a typical plot of the ratio $c_{A,t}/c_{A,t=0}$ versus time t for an experimental run, where c_A is the tracer concentration in the liquid pool. It is apparent that the model fits the experimental data well, and this agreement between theory and experiments supports the validity of this model for these experiments. It is, therefore, easy to forget that the dispersion coefficient evaluated by this method only illustrates the behaviour of the liquid pool. Therefore, the conditions inside the bed are not necessarily reflected by the dispersion coefficient.

In order to investigate the validity of the dispersion model in a packed bubble column, further dispersion experiments were conducted. Samples were taken at a sample point at approximately half the bed height. At this point, samples were taken at three different radial positions inside the bed: 10, 50 and 100 mm from the column wall ($r/R = 0.9, 0.5, 0$).

The results obtained from these trials are shown in Figs. 6–8 below. In the figures, the ratios between the

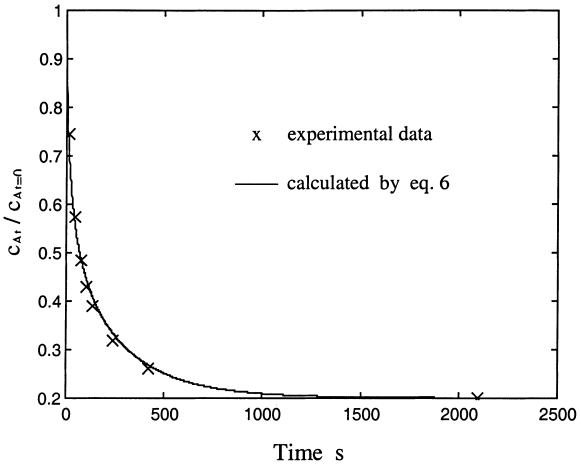

Fig. 5. Comparison of observed and calculated values of the ratio $c_{A,t}/c_{A,t=0}$ vs. the time t; $c_{A,t}$ is the pool concentration at time t and $c_{A,t=0}$ the initial pool concentration.

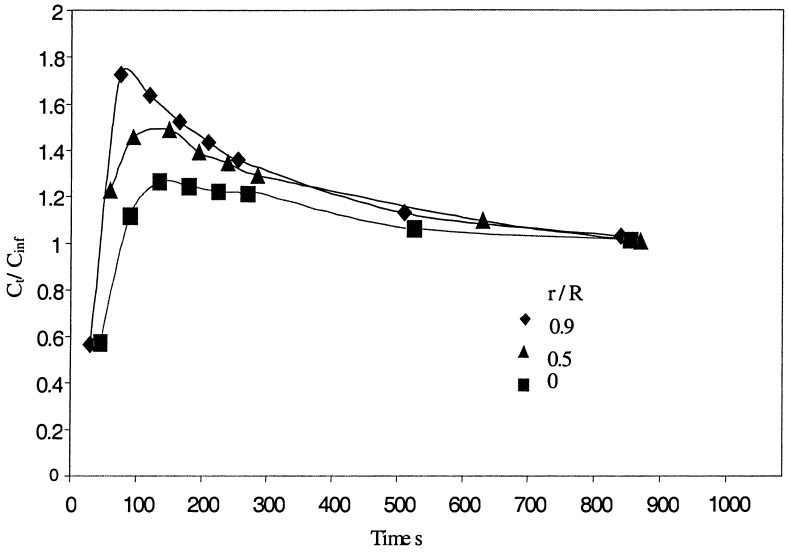

Fig. 6. Experimental data of the ratio C_t/C_{inf} at different radial positions plotted vs. time and at a distance of 0.6 m from the liquid pool. $U_G = 0.06$ m/s.

tracer concentration at time t and the tracer concentration at infinite time, C_t/C_{inf}, are plotted against time.

The figures represent three different gas velocities. In Fig. 6, the superficial gas velocity was approximately 0.06 m/s and the bubble column was operated in the bubble flow regime. The figure illustrates that the distribution of the tracer is dependent on the radial position. The tracer near the column wall is distributed faster than the tracer in the middle of the column; the tracer at $r/R = 0.5$ is distributed with a velocity between these two. Such trends can only be explained by the fact that the liquid flows upwards in the centre and downwards near the wall region. Similar behaviour in packed bubble columns has been observed and discussed by Katz [1]. This situation can also be compared to the conditions existing in empty bubble columns where the time-averaged liquid velocity profile shows a comparable rising liquid flow in the centre and a descending flow at the periphery.

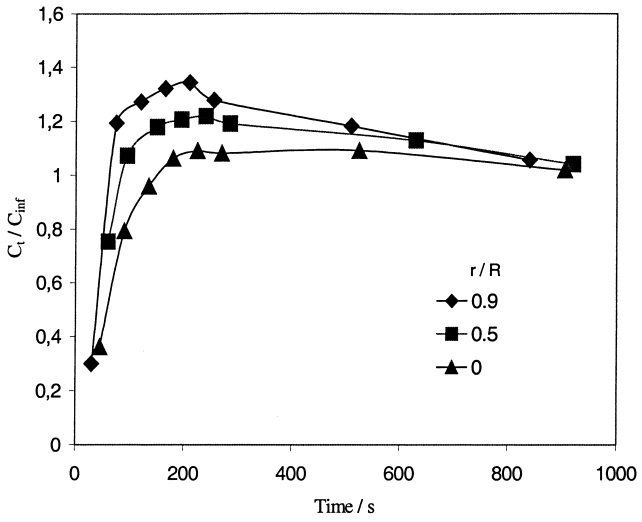

Fig. 7. Experimental data of the ratio C_t/C_{inf} at different radial positions vs. time and at a distance of 0.6 m from the liquid pool. $U_G = 0.09$ m/s.

It is apparent from the figures that the concentration gradients across the column cross-section decrease gradually when the gas velocity is increased. At a superficial gas velocity of approximately 0.07 m/s, there is a transition from bubble flow to pulsation flow. When the pulses rise upwards along the bubble column axis, each pulse increases the exchange of liquid elements in the radial direction. At approximately 0.14 m/s, a completely uniform radial concentration profile is achieved. This profile may be strongly connected to the sudden increase in the pulse frequencies at this gas velocity.

It can be concluded that the dispersion model in its simplest form, as given by Eq. (2), does not describe the conditions in the bed correctly. The model would be improved by considering the radial variations. However, it can be expected that Eq. (2) can be used when the radial variations disappear in the pulsation flow regime at higher pulse-frequencies. The experimental data shown in Fig. 8 ($U_G = 0.14$ m/s), is plotted in Fig. 9 and compared to tracer response curves calculated from Eq. (2). The response curve plotted with $E_L = 0.0028\,m^2/s$ corresponds to the evaluated value from the experiments. The figure shows that the dispersion model given by Eq. (2) does not fit the experimental data. Even if the dispersion coefficient is varied, there is a substantial disagreement between the model and the experimental data. These calculations indicate that mixing is not only dispersive in its character: the convective contribution is considerable in both the bubble flow regime and in the pulsation flow regime.

Finally, it must be emphasised that the concentration gradient in the radial direction in this work cannot be a result

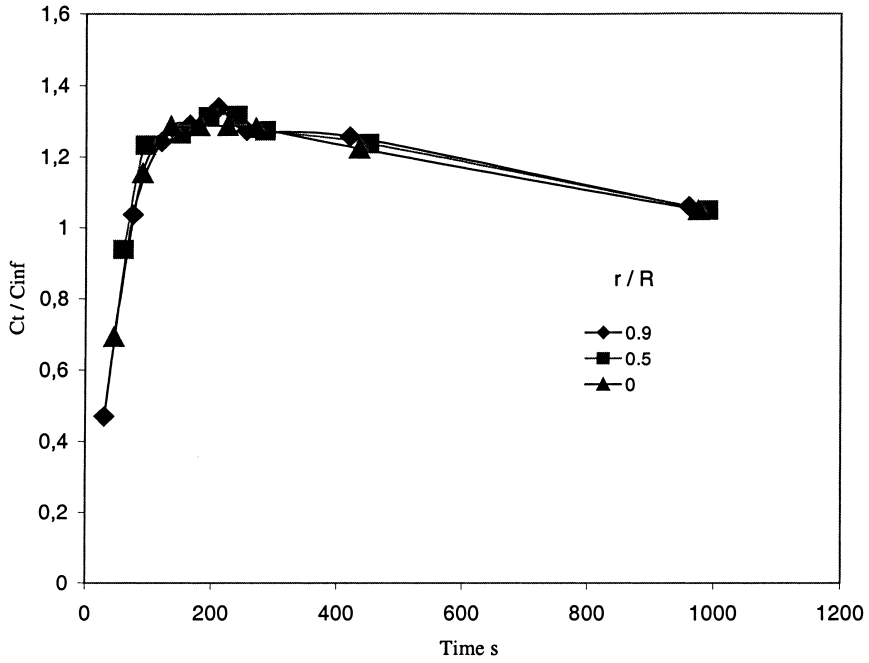

Fig. 8. Experimental data of the ratio C_t/C_{inf} at different radial positions vs. time and at a distance of 0.6 m from the liquid pool. $U_G = 0.135$ m/s.

of the maldistribution of tracer, since the tracer disperses quickly after injection and gives a uniform concentration in the liquid pool.

5. Modelling dispersion including internal convective liquid flow

From the discussion in Section 4, it is clear that the dispersion model cannot explain the physical behaviour of the RTD curves in Figs. 6–8. A more realistic model must include a convective contribution as well as a term describing the radial mixing behaviour. The disadvantage with this kind of model is the lack of experimental data regarding local liquid velocities. In spite of this, a simplified mechanistic mixing model is proposed below. The purpose of this model is to demonstrate the different effects of circulation flow and turbulence on mixing. Similar approaches have been used earlier by Wilkinson et al. [18] and more recently by Degaleesan et al. [19,20] for an empty bubble column to explain the dispersion in empty bubble columns at elevated pressures. In the present study, the liquid pool above the packed bed and the region just above the gas sparger are assumed to be well-stirred. These two volumes are, therefore, considered as two perfectly-mixed tanks.

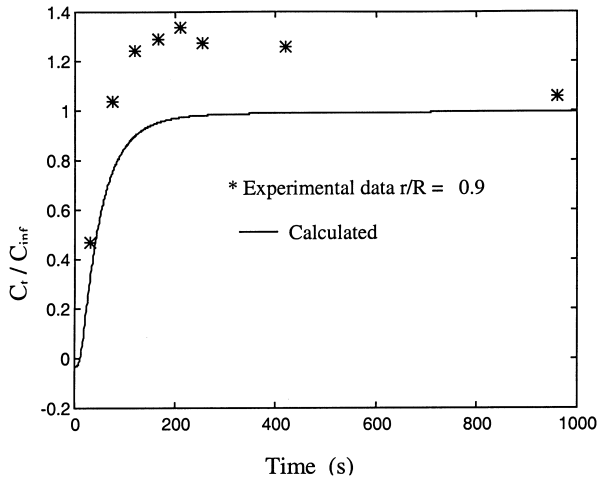

Fig. 9. Observed and calculated values of the ratio C_t/C_{inf} at a position 0.6 m from the liquid pool. The calculated concentration profile is predicted by the one-dimensional dispersion model (Eq. (2)). $U_G = 0.13$ m/s.

According to Fig. 10, it is assumed that there are two separate liquid flow regions: the upflow region in the middle of the column and the downflow at the wall with the liquid velocities u^d and u^u, respectively. The radial exchange of tracer between the upflow and downflow regions are accounted for by the exchange coefficient, K. The turbulent mixing is represented by the dispersion coefficient E. The transport equations for the two regions are given by

$$\text{Downflow} \quad \frac{\partial C^d}{\partial t} = E^d \frac{\partial^2 C^d}{\partial x^2} - u^d \frac{\partial C^d}{\partial x} - \frac{K}{A_d \varepsilon_L}(C^u - C^d) \tag{9}$$

$$\text{Upflow} \quad \frac{\partial C^u}{\partial t} = E^u \frac{\partial^2 C^u}{\partial x^2} + u^u \frac{\partial^2 C^u}{\partial x} + \frac{K}{A_u \varepsilon_L}(C^u - C^d) \tag{10}$$

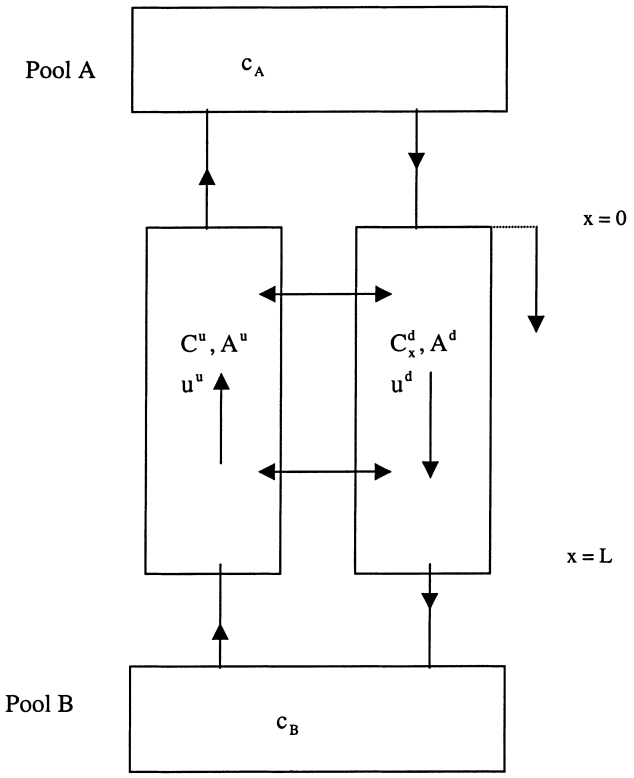

Fig. 10. A circulating packed bubble column with a liquid pool.

where ε_L is the liquid holdup in the packed section of the column; C^u the tracer concentration in the upflow; C^d the tracer concentration in the downflow; c_A, c_B the tracer concentrations in the liquid pools; E^u, E^d the dispersion coefficients in the upflow and downflow sections; and A^u, A^d the cross sectional areas in the upflow and the downflow, respectively.

In this case, it is assumed that there is only convective mass transport between the pools and the boundaries. The mass transport between the boundaries and the packed section is due to dispersion and convection. The boundary conditions can, therefore, be described by Danckwerts conditions and, for a pulse injection of the tracer in the liquid pool above the packed bed we get

$$\text{Downflow} \quad u^d c_A = u^d C^d_{x=0} - E^d \frac{\partial C^d_{x=0}}{\partial x} \quad \text{at} \quad x = 0 \text{ and } t > 0 \tag{11}$$

$$\frac{\partial C^d_{x=L}}{\partial x} = 0 \quad \text{at} \quad x = L \text{ and } t > 0 \tag{12}$$

$$C^d(x, 0) = 0 \quad \text{for } x > 0$$

$$\text{Upflow} \quad u^u c_B = u^u C^u_{x=L} + E^u \frac{\partial C^u_{x=L}}{\partial x} \quad \text{at} \quad x = L \text{ and } t > 0 \tag{13}$$

$$\frac{\partial C^d_{x=0}}{\partial x} = 0 \quad \text{at} \quad x = 0 \text{ and } t > 0 \tag{14}$$

$$C^u(x, 0) = 0 \quad \text{for } x > 0$$

$$\text{Liquid pool A} \quad c_A = C_0 \quad \text{at } t = 0$$

$$C^u A^u u^u = c_A A^d u^d + v_A \frac{\partial c_A}{\partial t} \tag{15}$$

$$\text{Liquid pool B} \quad c_B = 0 \quad \text{at } t = 0$$

$$C^d A^d u^d = c_B A^u u^u + v_B \frac{\partial c_B}{\partial t} \tag{16}$$

where v_A, v_B are the liquid volumes of the pools.

It is assumed that the average liquid velocities are equal in both directions, i.e. $u^d = u^u$, and consequently, the boundary between the two regions is determined by the necessary fact that $A^u = A^d$. Thus, the position of zero velocity, where the positive upflow changes to downflow, will be $r/R = 1/\sqrt{2}$. This position of time-averaged zero velocity is well documented for empty bubble columns (Chen et al. [21], Dudukovic et al. [22], Walter and Blanch [23]). This assumption was made in this work although no such data is available in the literature for packed bubble columns.

The equations have been solved with different values of u, E and K by using an implicit backward Euler method with a time interval of 1 s and a length interval of 0.01 m. No parameter estimation has been performed. This is due to the fact that too many independent and unknown parameters have to be taken into account.

Figs. 11–13 show the results of several simulation trials and demonstrate the influence of the exchange coefficient K. Experimental data at $U_G = 0.06$ m/s is also plotted. Firstly, it can be concluded that increasing the exchange coefficient decreases the rate of mass transport from the liquid pool to the packed bed and decreases the dispersion. The observed sudden reduction of the overall liquid dispersion coefficient

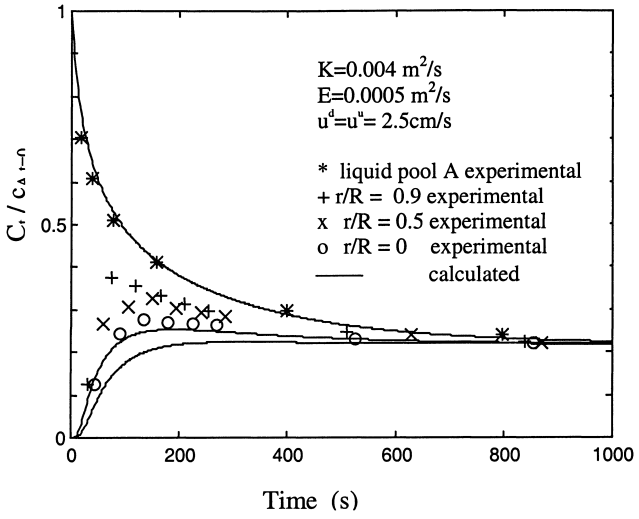

Fig. 11. Dynamic tracer response profiles, $C_t/c_{A,t=0}$ in the upflow, downflow ($x = 0.6$ m) and the liquid pool calculated from Eqs. (9) and (10). The predicted values are compared to experimental data. $U_G = 6$ cm/s.

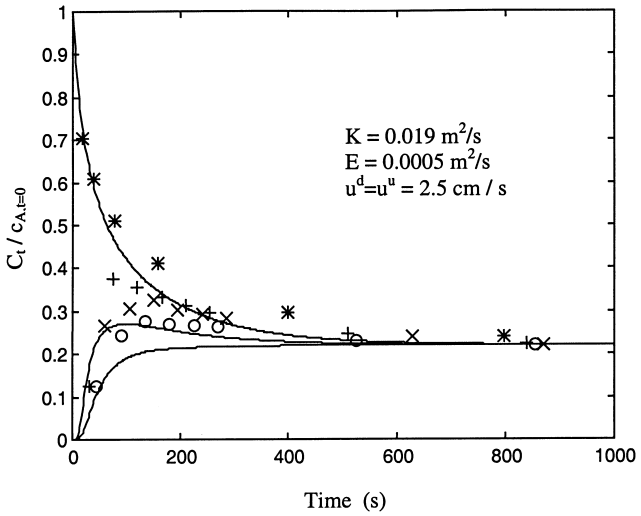

Fig. 12. Dynamic tracer response profiles, $C_t/c_{A,t=0}$ in the upflow, downflow ($x = 0.6$ m) and the liquid pool calculated from Eqs. (9) and (10). The predicted values are compared to experimental data. $U_G = 6$ cm/s. Symbols same as in Fig. 11.

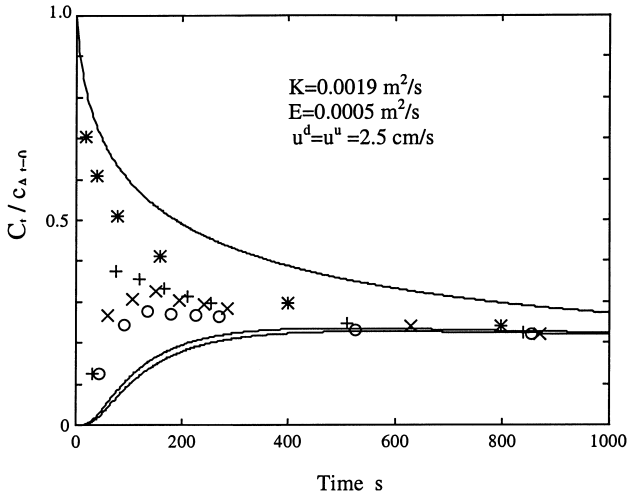

Fig. 13. Dynamic tracer response profile, $C_t/c_{A,t=0}$ in the upflow, downflow ($x = 0.6$ m) and the liquid pool calculated from Eqs. (9) and (10). The predicted values are compared to experimental data. Symbols same as in Fig. 11. $U_G = 6$ cm/s.

in Fig. 4 can, thus, be explained by a larger exchange of liquid elements. This increase is clearly connected to the formation and the nature of the pulses that are formed at this gas velocity. A further increase of the exchange coefficient will cause a uniform radial concentration profile. A reduction of K means that the maximum point of the concentration profile curves also reaches a higher value as a consequence of the larger 'all-over dispersion coefficient'.

It is also evident that the efforts to achieve good agreement between the model calculations and the experimental data from the packed section failed. Despite several variations of u, E and K, the maximum points of the experimental tracer distribution curves could not be obtained from these calculations. The reasons for this are discussed below.

The calculated concentration as a function of the time at a distance of 0.01 m from the upper boundary is shown in Fig. 14. A considerable time is required to achieve a concentration in the region close to the boundary that is the same as in the liquid pool. Such slow mixing between the liquid pool and the packed bed close to the boundary may be unrealistic. This implies that the Danckwerts boundary condition at the pool, Eqs. (12) and (14), are not suitable for this

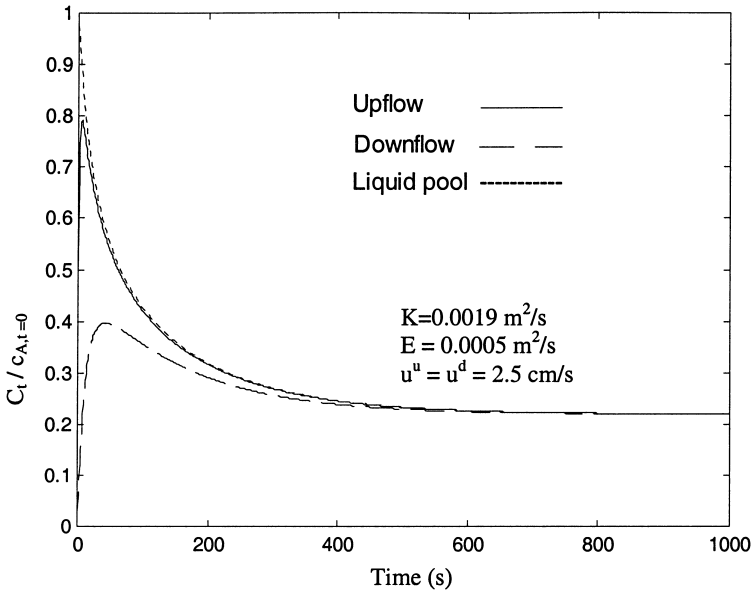

Fig. 14. Calculated tracer concentration $C_t/c_{A,t=0}$ as a function of time in the packed bed at a distance of 1 cm from the upper boundary. Eqs. (9) and (10) and the Danckwerts boundary conditions Eqs. (11)–(16).

application. It is also doubtful whether Eqs. (15) and (16) describe the conditions in a correct way. These equations predict a concentration step between the liquid pool and the boundary. It is more probable that there is extremely rapid mixing of the tracer in the liquid pool, making it reasonable to assume that the concentration of the tracer at the boundary and in the liquid pool are equal.

The Danckwerts boundary conditions have been extensively discussed in the literature. As pointed out by Nauman and Mallikarjun [24], the Danckwerts boundary conditions predict unrealistic concentration profiles in packed beds when the dispersion coefficient is controlled primarily by convection rather than diffusion. Eqs. (12) and (14) show a zero concentration gradient at $x = 0$ for the upflow and at $x = L$ for the downflow. The assumption of a pure convective mass transport between the upper liquid pool and the upflow, expressed by Eq. (12), may be seriously questioned. The zero gradient at the reactor outlet as suggested by Danckwerts [25] results from concentration at the end of the packing being higher than in the exit stream. In this situation, the mass balance is similar to Eq. (11) and shows that if $\partial C/\partial x$ is positive the concentration will pass a minimum somewhere in the reactor. If $\partial C/\partial x$ is negative the concentration in the exit stream will be greater than at the end of the packing. Since either of these two cases can arise, the concentration gradient at the outlet boundary is zero. In this work, the second situation actually occurs; the concentration of tracer in pool A is higher than the concentration of tracer at the outlet of the upflow stream. The same situation may also arise at the lower boundary. The necessary conditions for a longitudinal back dispersion between the pools and the inlet streams to the pools are, therefore, fulfilled. For this reason some calculations were performed assuming instantaneous mixing in the pools and the same concentration of the tracer at the boundaries as in the pools. Also the mass transport between the boundaries and the packed section was considered to be a result of both dispersion and convective streams. These assumptions result in the following boundary conditions:

$$x=0 \text{ and } t > 0 \quad -C^{\mathrm{d}}u^{\mathrm{d}}A^{\mathrm{d}}\varepsilon + C^{\mathrm{u}}u^{\mathrm{u}}A^{\mathrm{u}}\varepsilon + A^{\mathrm{d}}\varepsilon E^{\mathrm{d}}\frac{\partial C^{\mathrm{d}}}{\partial x} + A^{\mathrm{u}}\varepsilon E^{\mathrm{u}}\frac{\partial C^{\mathrm{u}}}{\partial x} = v_{\mathrm{A}}\frac{\partial c_{\mathrm{A}}}{\partial t} \tag{17}$$

$$x = L \text{ and } t > 0 \quad C^{\mathrm{d}}u^{\mathrm{d}}A^{\mathrm{d}}\varepsilon - C^{\mathrm{u}}u^{\mathrm{u}}A^{\mathrm{u}}\varepsilon - A^{\mathrm{d}}\varepsilon E^{\mathrm{d}}\frac{\partial C^{\mathrm{d}}}{\partial x} - A^{\mathrm{u}}\varepsilon E^{\mathrm{u}}\frac{\partial C^{\mathrm{u}}}{\partial x} = v_{\mathrm{B}}\frac{\partial c_{\mathrm{B}}}{\partial t} \tag{18}$$

$$t \geq 0 \quad c_{\mathrm{A}} = C^{\mathrm{d}}_{x=0} = C^{\mathrm{u}}_{x=0} \quad \text{and} \quad c_{\mathrm{B}} = C^{\mathrm{d}}_{x=L} = C^{\mathrm{u}}_{x=L} \tag{19}$$

The results of the calculations are shown in Figs. 15–17. A faster response is now achieved (c.f. Figs. 16–17) and small maximum points can be detected both for the upflow and downflow streams in Fig. 15. However, the level of the maximum point is still too low. One reasonable explanation for this is a faster distribution of the tracer and a larger mixing in the upper part compared to the lower regions of the bed.

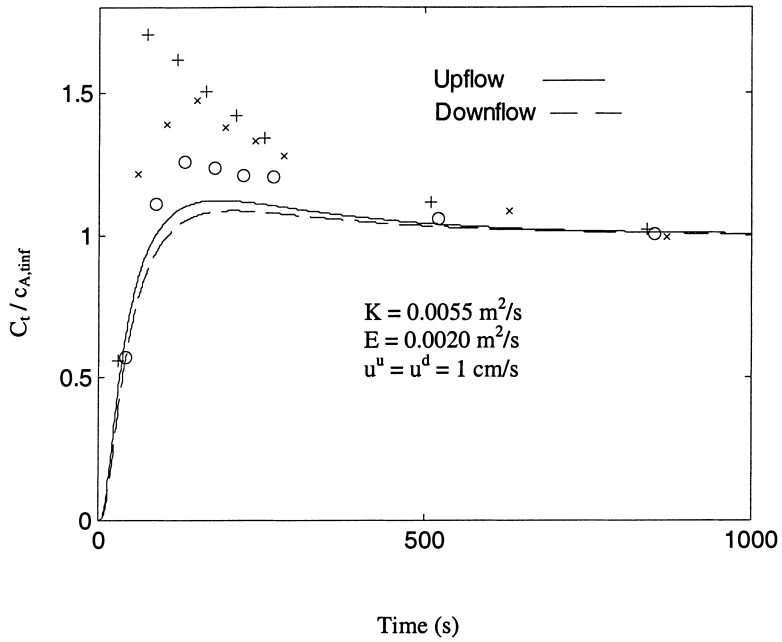

Fig. 15. A comparison between calculated and experimental tracer profiles, C_t/C_{inf} at a distance of 0.6 m from the pool. Eqs. (9) and (10) and the modified boundary conditions Eqs. (17)–(19). Symbols same as Fig. 11.

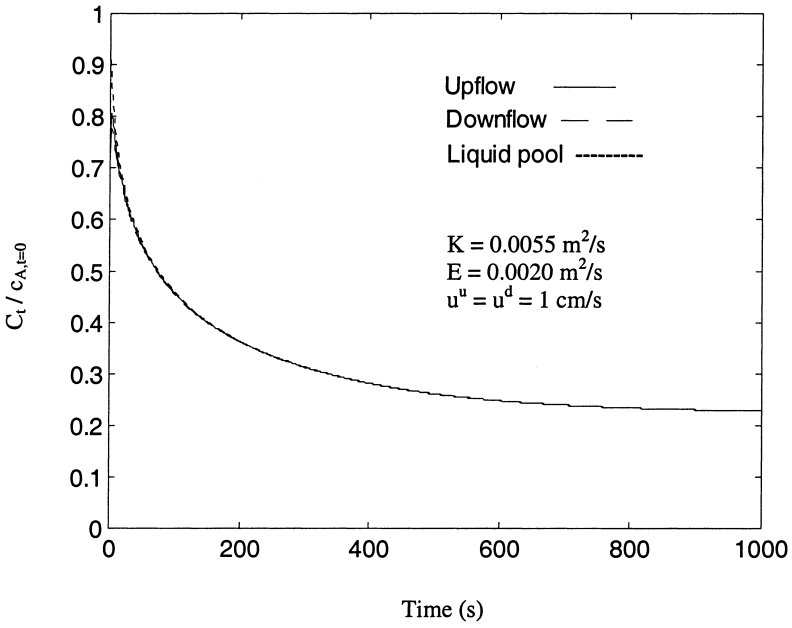

Fig. 16. Calculated tracer concentration in the bed, $C_t/c_{A,t=0}$ as a function of time at a position of 1 cm below the upper boundary. Eqs. (9) and (10) and the modified boundary conditions Eqs. (17)–(19).

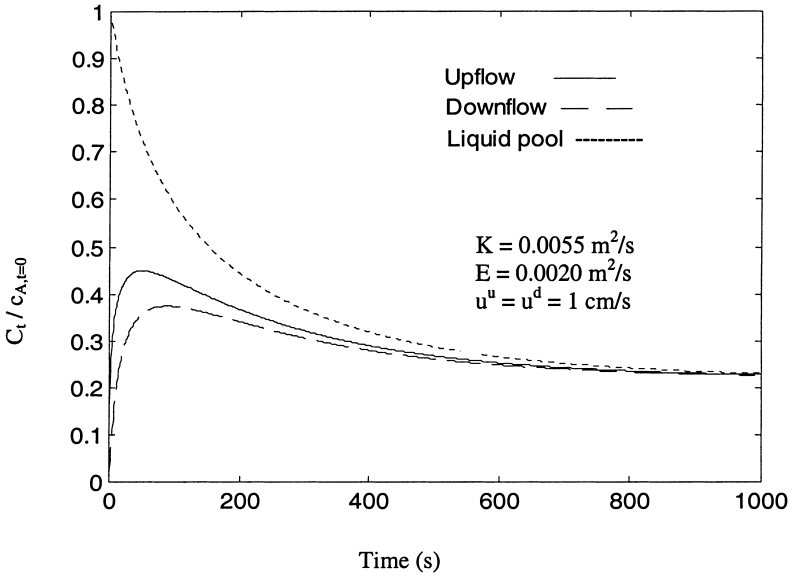

Fig. 17. Calculated tracer concentration, $C_t/c_{A,t=0}$ as a function of time in the packed bed at a distance of 1 cm from the upper boundary. Eqs. (9) and (10) and the Danckwerts boundary conditions, Eqs. (11)–(16).

6. Conclusions

- It is observed that the gas holdup increases at increased superficial gas velocity. The diameter of the packed bubble column does not influence the gas holdup.
- Two flow regimes are observed: bubble- and pulsation flow. The pulsation flow regimes starts at U_G approximately 0.07 m/s. In both regions, the one dimensional axial dispersion coefficient increases with increasing gas velocity. However, the radial mixing shows a substantial increase in the pulsation flow regime. As a result of this, the dispersion coefficient reduces suddenly at the transition point between the bubble flow and the pulsation flow regime.
- There is a non-uniform liquid velocity distribution in the radial direction in a packed bubble column. This liquid circulation comprises an upward flow in the column core and a downward flow along the wall.
- The one-dimensional dispersion model does not correctly predict the tracer concentration profile inside the bed when

a pulse injection is used. This is due to the convective liquid flows and poor radial mixing. The dispersion model also gives a poor description at higher gas velocities, when radial mixing in the pulse flow region equalises the concentration gradient.

Acknowledgements

The support by Dr. Johan Wanngård and Dr. Mats Nyström, EKA Chemicals (Sweden) is gratefully acknowledged.

References

[1] M.B. Katz, Theor. Foundations Chem. Eng. 12 (1978) 496.
[2] Y.T. Shah, G.J. Stiegel, M.M. Sharma, AIChE J. 24 (1978) 369.
[3] G.J. Stiegel, Y.T. Shah, Ind. Eng. Chem. Proc. Des. Dev. 16 (1977) 37.
[4] M. Abraham, S.B. Sawant, Chem. Eng. J. 43 (1990) 95.
[5] K. Niranjan, V.G. Pangarkar, Chem. Eng. J. 29 (1984) 101.
[6] J.L. Turpin, R.L. Huntington, AIChE J. 13 (1967) 1196.
[7] J.B.L.M. Campos, J.R.F.A. Guedes de Carvalho, Chem. Eng. Sci. 47 (1992) 4063.
[8] H.S. Carslaw, J.C. Jaeger, Conduction of Heat in Solids, Oxford University Press, Oxford, 1959.
[9] B.N. Sahay, M.M. Sharma, Chem. Eng. Sci. 28 (1973) 2245.
[10] P.A. Ramachadran, R.V. Chaudari, Three-Phase Catalytic Reactors, Gordon and Breach, London, 1983.
[11] V.W. Heilman, H. Hofman, in: Proceedings of the Fourth European Symposium on Chemical Reactor Engineering, Brussels, Belgium, 1968.
[12] H. Hofmann, Chem. Eng. Sci. 14 (1961) 193.
[13] K.B. Gelder, K.R. Westerterp, Chem. Eng. Technol. 13 (1990) 27.
[14] A.J. Carleton, R.J. Flain, J. Rennie, F.H.H. Valentin, Chem. Eng. Sci. 22 (1967) 1839.
[15] P. Magnussen, V. Schumacher, in: Proceedings of the Fifth International Symposium on Chemical Reactor Engineering, Vol. 65, 1978, 337 pp.
[16] C.J. Hoogendorn, J. Lips, Can. J. Chem. Eng. 43 (1965) 125.
[17] S. Stemmerding, Chem. Eng. Sci. 14 (1961) 209.
[18] P.M. Wilkinsson, H. Haringa, H.P.A. Stokeman, L.L. van Dierendonck, Chem. Eng. Sci. 48 (1993) 1785.
[19] S. Degaleesan, S. Roy, S.B. Kumar, M.P. Dudukovic, Chem. Eng. Sci 51 (1996) 1967.
[20] S. Degaleesan, M.P. Dudukovic, B.A. Toseland, B.L. Bhatt, Ind. Eng. Chem. Res. 36 (1997) 4670.
[21] R.C. Chen, J. Reese, L.S. Fan, AIChE J. 40 (1994) 1093.
[22] M.P. Dudukovic, N. Devanathan, R. Holub, Revue de L'Institute Francais du Petrole 47 (1991) 439.
[23] J.F. Walter, H.W. Blanch, Chem. Eng. Comm. 19 (1983) 243.
[24] E.B. Nauman, R. Mallikarjun, Chem. Eng. J. 26 (1983) 231.
[25] P.V. Danckwerts, Chem. Eng. Sci. 1 (1953) 1.